ANNALS OF GEOPHYSICS, 66, 5, PA533, 2023; doi:10.4401/ag-9000
OPEN ACCESS

Spatial and Temporal Analysis of Carbon Dioxide Concentrations over Italy by means of OCO-2 Satellite Data Series

Vito Romaniello[1], Claudia Spinetti[1], Alessandro Piscini[1]

(1) Istituto Nazionale di Geofisica e Vulcanologia, Via di Vigna Murata 605, 00143 Roma, Italy

Article history: received June 20, 2023; accepted January 1, 2024

Abstract

Carbon dioxide is a greenhouse gas with sink and source related to natural cycles and anthropic activities. OCO-2 is a NASA carbon dioxide dedicated mission launched in 2014 aimed to measure the CO_2 concentrations in the atmosphere by recording sunlight reflected off the Earth and provides, at the state of the art, the highest spatial resolution for mapping CO_2 at global scale. In this work, for the first time, we statistically analyse 8 years of OCO-2 acquisitions over Italian territory, obtaining the main trend and the seasonal behaviour of CO_2 over land. After data reprocessing and compensating on temporal frequency of OCO-2 acquisitions over Italy, a mean of 21 ppm of increment in the period from 2015 to 2022 has been found. In the data time series, we also noticed a significant acceleration in the trend between 2019 and 2020 and a return to average values of the trend after the COVID19 pandemic lockdown. In addition, such trends have been compared with those achieved by the European Centre for Medium Range Weather Forecasts (ECMWF) model. The data time series was also used to perform a spatial analysis of areas characterized by lower/higher CO_2 concentrations to detect sinks/sources in Italy due to the land use. The analysis reveals that the North Italian regions, with more population and industries, are the source of CO_2; moreover, the fundamental role of vegetation as a sink of CO_2 is confirmed.

Keywords: Carbon dioxide; OCO-2 mission; ECMWF; Spatial and temporal analysis; Italy

1. Introduction

The carbon dioxide gas (CO_2) represents the most important atmospheric contributor to the warming of the troposphere as greenhouse gases (GHG). CO_2 greenhouse power is low, compared to other greenhouse gas atmospheric components such as CH_4, but it accounts for about half of the anthropogenic contribution to the greenhouse effect [Masson-Delmotte et al., 2021]. The industrial revolution (year 1760) has been possible thanks to the increasing availability of energy based on fossil fuels such as coal, oil and natural gas that are non-renewable energy resources [Bartoletto et al., 2008]. After the second world war, the worldwide rise in fossil fuel consumption has immensely increased CO_2 emissions. In fact, considering pre-industrial times, CO_2 has risen by 46% in the atmosphere [WMO, 2019]. This rise of CO_2 levels is caused by fossil fuel combustion with a substantial contribution from land use change.

Since 1992, the establishment of the United Nations Framework Convention on Climate Change [UNFCCC, 2023] recognized the anthropogenic role in climate change. The Intergovernmental Panel for Climate Change (IPCC) and the Conference of Parties (COP) have undertaken many actions, even if global emissions of greenhouse gases have not yet been curbed [Petrescu et al., 2020]. The Paris Agreement (PA) defines the Nationally Determined Contributions (NDCs) and targets progress of decal emission reduction efforts as tracking on the basis of regular updates to national greenhouse gas inventories, referred to as bottom up estimates. However, only top-down atmospheric measurements can provide observation-based evidence of emission trends. The reliable quantification of GHG emissions to the latest scientific standards in support of the Paris Agreement is urgent [WMO, 2019]. Globally, fossil fuel emissions grew at a rate of 1.5 % yr^{-1} for the decade 2008-2017 and account for 87 % of the anthropogenic sources in the total carbon budget [Le Quéré et al., 2018]. In contrast, global emissions from land use change were estimated from bookkeeping models and land carbon models to be approximately stable in the same period, albeit with large uncertainties [Le Quéré et al., 2018]. The Earth Observation (EO) missions can provide a useful way to quantify at global but also at national scale the CO_2 emissions. The European ENVIronmental SATellite (ENVISAT), 2002-12, was the first space borne mission to measure XCO2 and XCH4 by using the SCIAMACHY instrument [Schneising et al., 2013] followed by the IASI instrument [Del Bianco et al., 2013]. The first space mission totally dedicated to monitor CO_2 is the Japanese GOSAT launched in 2009 with an on board thermal and near-infrared Fourier transform spectrometer that delivers column-averaged dry-air mole fractions of CO_2 denoted XCO2 product [Yoshida et al., 2013; Buchwitz et al., 2015]. Afterwards, the NASA OCO-2 space mission was launched in 2014 [Crisp et al., 2012]. The TanSat Chinese carbon dioxide satellite, launched in 2016, adds at global scale more XCO2 data. At local scale the first maps of CO_2 emitted from natural volcanic and industrial point sources have been obtained by using airborne AVIRIS hyperspectral instrument, thanks to the meter spatial resolution of the images and the instrumental sensitivity of the SWIR bands [Spinetti et al., 2008; Thorpe et al., 2017]. Also satellite hyperspectral sensors such as the PRISMA mission, launched on 2019, have demonstrated their ability in obtaining such important achievement [Loizzo et al., 2018; Cusworth et al., 2021; Romaniello et al., 2021]. A new constellation CO_2 satellite imagery sensor (CO2M) of the European Space Agency (ESA) is under construction in the framework of the Copernicus program. The CO2M will carry on board a broad-swath imaging grating spectrometer for CO_2, CH_4, NO_2, and aerosols from January 2026 onward.

In this work, the Orbiting Carbon Observatory 2 (OCO-2) acquisitions have been analysed at national scale, for the first time over the Italian territory, covering a temporal range from 2014 to 2022 years, highlighting sources and sinks of CO_2.

2. Data and Methodology

The OCO-2 space mission started delivering XCO2 data in 2014; the instrument on board is composed by a three-channel imaging grating spectrometer and yields the spatial structure of XCO2 variations across cities allowing the identification of CO_2 emissions from localised sources [Nassar et al., 2017; Schwandner et al., 2017] thanks to the highest spatial resolution in the framework of the CO_2 dedicated space missions. The OCO-2 instrument utilises a push broom scanning technique with a swath width of about 10 km and spatial resolution of 1.29 km (cross-track) and 2.25 km (along-track); the satellite revisit time is 16 days.

The dataset used in this study is composed of 875 OCO-2 passes acquired over Italian territory in the period September 8, 2014 – December 29, 2022. Specifically, the standard products "OCO2_L2_Standard" were processed [OCO-2, 2023]. With the aim to achieve information on the entire Italian territory, an algorithm has been implemented to perform temporal and spatial analyses at different scales. Figure 1 shows the scheme of the processing chain providing as output the temporal trend of CO_2 concentrations and the land distribution map of sinks and sources at several spatial resolutions. Firstly, a sea/land mask was applied in order to consider only acquisitions on Italian land; then, a spatial grid is created at three different scales (0.10, 0.15 and 0.20 deg). The need to consider regular spatial grids is due to the acquisition geometry of OCO-2, characterized by very narrow swaths (< 8 km). The satellite sounding within each ground pixel is assigned to that pixel and, in case of two or more soundings, their mean value is considered. It is clear that, for finer spatial resolutions, the OCO-2 soundings are more representative of the associated areas but small pixels may not completely cover the territory. With the aim to obtain the temporal series (first output in Figure 1), the mean value of CO_2 concentration, for each OCO-2 passage, is calculated averaging the pixels' values of the distribution map. Regarding the spatial distribution analysis, the difference between values of

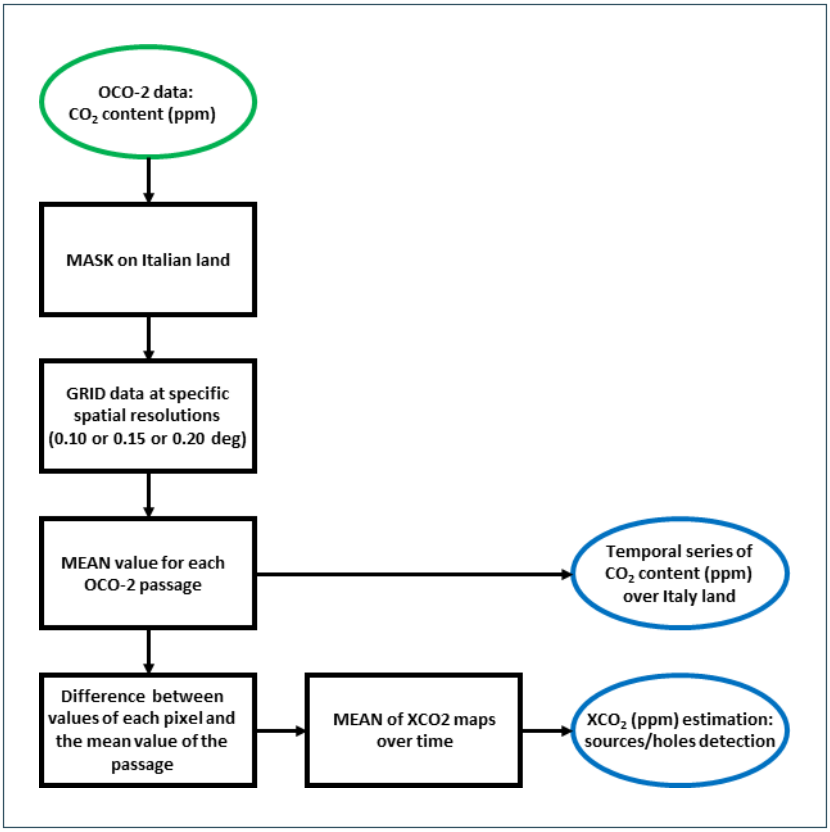

Figure 1. Scheme of the processing algorithm to analyse OCO-2 data.

each pixel and the mean value of the passage is computed to obtain XCO2 values related to each satellite acquisition. Finally, the XCO2 maps of all acquisitions are averaged in order to obtain the map of sinks/sources distribution that takes in account the entire period of the dataset employed (second output in Figure 1).

The processing chain, analysing a large dataset, is able to provide the temporal series of CO_2 concentrations on a specific area of interest and the maps representing spatial areas characterized by XCO2 values under/above the average value of the entire considered territory.

3. Results and Discussion

3.1 Temporal analysis

The temporal analysis is performed calculating the average value of OCO-2 soundings for each satellite crossing over Italy. The time series is obtained following the processing chain shown in Figure 1 and the temporal trend is depicted in Figure 2 (black points). Moreover, the measurements are interpolated (by means of a polynomial interpolation) to obtain the fitting trend (red line). This allows us to appreciate the typical seasonal variability and the continuous increase of the CO_2 concentrations during the 8 years analysed.

The seasonal variability is clearly characterized by maximum and minimum values in the periods March-April and August-September of each year, respectively. In Table 1 the yearly mean values are reported to evaluate the increasing of CO_2 concentrations over the time. The error results from the error propagation formula by normalizing the standard deviation to the square root of the number of measurements.

The mean values spanned from a minimum of about 396 ppm to a maximum of about 417 ppm in the years 2015 and 2022, respectively. This allows us to estimate an increasing trend of about 3 ppm/year. We also noticed a significant rate in the trend between 2019 and 2020, with an increase of about 6 ppm, and a return to average values of the trend in 2021 and 2022. This behaviour coincides in time with the COVID19 pandemic lockdown in Europe, which occurred in the first months of 2020, slowing down the increment trend.

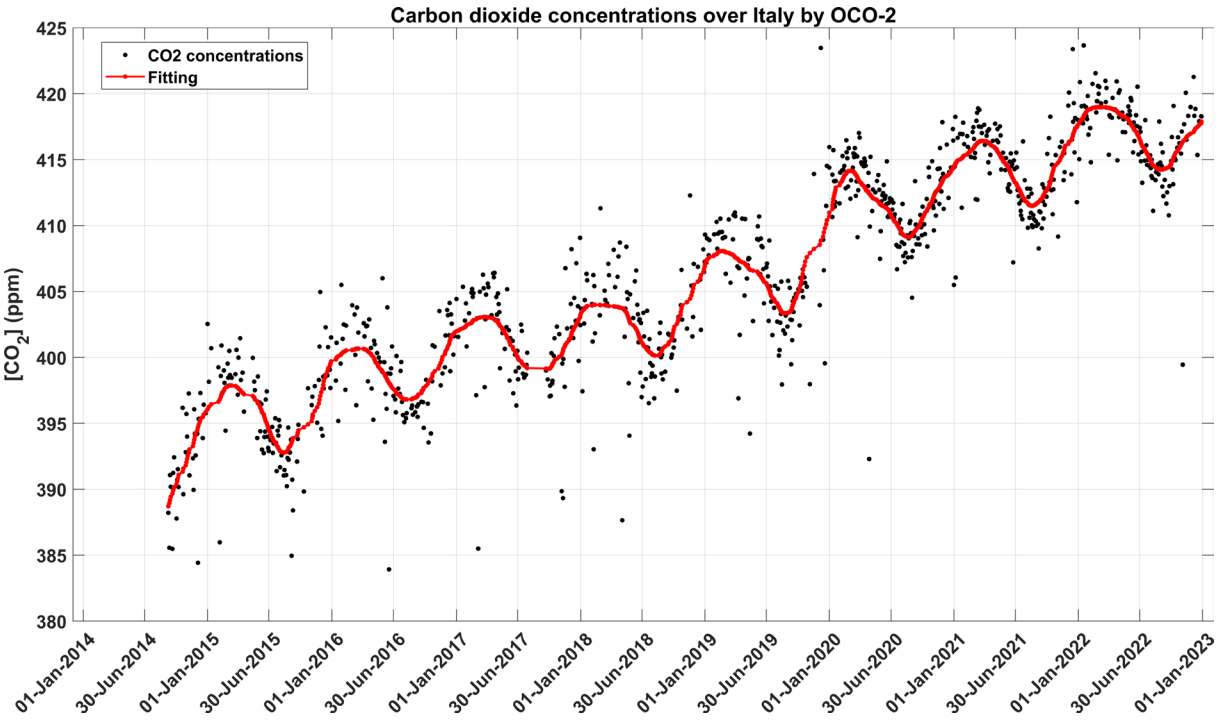

Figure 2. Average values of CO_2 concentrations (ppm) for each OCO-2 satellite crossing over Italy (black dots) and fitting trend (red line).

Year	Mean value (ppm)	Error (ppm)
2015	395.86	±0.38
2016	399.05	±0.36
2017	401.55	±0.40
2018	402.55	±0.39
2019	406.15	±0.40
2020	411.98	±0.25
2021	414.28	±0.26
2022	416.94	±0.25

Table 1. Mean CO_2 concentrations on Italian land for each year.

In order to evaluate the reliability of the CO_2 trend derived from OCO-2 data, the estimations of gas concentrations by the European Centre for Medium Range Weather Forecasts (ECMWF) database have been considered for the Italian territory. The ECMWF Carbon Dioxide dataset is part of the project focused on long-lived greenhouse gases: CO_2 and CH_4 [Agustí-Panareda et al., 2014; Massart et al., 2014]. This is the latest global Atmospheric Composition (AC) reanalysis dataset by the Copernicus Atmosphere Monitoring Service (CAMS). It consists of time-coherent three-dimensional fields, including aerosols and chemical species, via separate CAMS Global Greenhouse Gas Reanalysis (EGG4). The CAMS reanalysis was produced using 4DVar data assimilation in the Cycle 42r1 of ECMWF's Integrated Forecasting System (IFS) atmospheric model, with 60 hybrid sigma/pressure vertical levels,

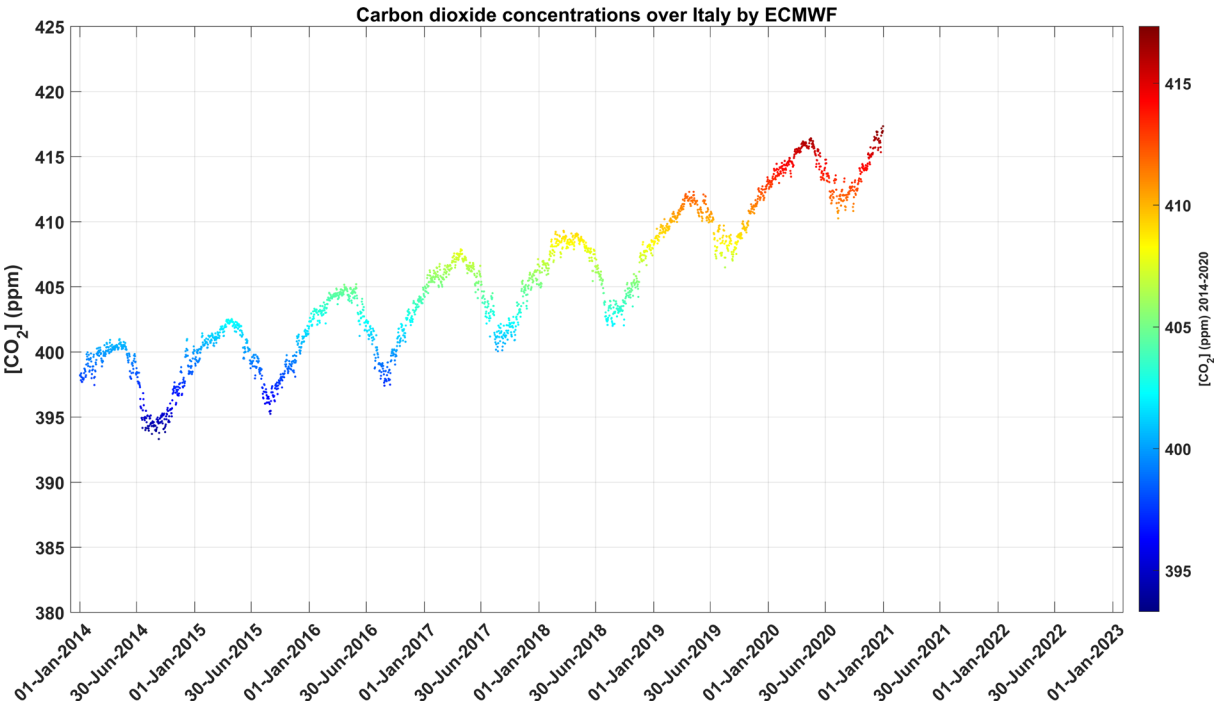

Figure 3. Trend of CO_2 (ppm) concentrations modelled by the ECMWF over Italy in the period 2014-2020.

with the top level at 0.1 hPa. The CAMS EGG4 reanalysis dataset covers the period 2003-2020. The fields were interpolated from their native representation to a regular grid of 0.75°x0.75° lat/lon. Generally, the data are available on a sub-daily and monthly basis and consist of 48 h analyses and forecasts, initialized daily by analyses at 00 UTC.

The CO_2 time series were extracted from 2014 to 2020 over an area that includes Italy; a land/sea mask has also been applied, with the same spatial resolution of the analysed data, to consider only the land pixels. The trend is depicted in Figure 3.

Table 2 reports the ECMWF maximum and minimum derived values for each year; the uncertainty is about $\pm$ 0.1 ppm calculated, as for OCO-2 data, applying the error propagation formula. The maximum value ranges from about 403 ppm to about 416 ppm estimated for the years 2015 and 2020, respectively; the minimum value increases from about 395 ppm to 411 ppm. The trend over Italy derived by ECMWF data is similar to the trend derived by OCO-2 data; in particular, the average growth rate results of about 2.9 ppm/year which is comparable with those obtained by OCO-2 analysis, despite the different spanning of the time series.

Year	Max value (ppm)	Min value (ppm)
2015	402.5	395.3
2016	405.2	397.4
2017	407.9	400.1
2018	409.2	402.0
2019	412.3	407.0
2020	416.3	410.7

Table 2. Maximum and minimum of ECMWF CO_2 concentrations estimated for each year in the period 2015-2020.

Despite the application of regulation in reducing the fossil fuel combustion (the first factor contributing to CO_2 emissions) in Italy (Table 3), the increasing trend has not inverted.

Category	2016	2017	2018
Energy: fuel combustion	346.475	341.329	337.529

Table 3. Summary of emission trends by energy source (Gg CO_2 equivalent) [ISPRA, 2018].

This may suggest that the countries in the world that have inverted the trend are too few to see effects in the virtuous countries, but also the important role of land use change in Italy, as a second factor contributing to CO_2 emissions [Corona et al., 2012; Solazzo et al., 2016]. Changes in the land surface (vegetation, soils, water) resulting from human activities are well described by IPCC [2007].

3.2 Spatial analysis – Sinks and Sources

The spatial analysis was performed at different ground resolutions also to understand the potential of OCO-2 data to detect and characterize sources/sinks at high spatial resolution. Figure 4 (left column) shows the XCO2 spatial distribution at three resolutions: 0.10, 0.15 and 0.20 deg; colour bars indicate the average of differences in the CO_2 concentration over time (see also Figure 1 for the processing algorithm). With the pixel size increasing, the narrow OCO-2 swaths are considered representative of larger areas, leading to a more homogeneous XCO2 distribution. Moreover, an index representing the sampling rate of satellite data was introduced in order to normalize the OCO-2 passes over Italy. The Sampling Index (ranging from 0 to 1) is calculated as the ratio between the number of acquisitions for each pixel and the maximum number of acquisitions for a single pixel in the entire period (2015-2022). So, this index provides information on the quality of the XCO2 spatial estimations (Figure 4, right column).

The XCO2 concentration maps clearly highlight the characterization of areas which determine an increase or a reduction of CO_2 at local scale. Furthermore, with the aim of merging information from different OCO-2 passes and reducing possible outliers, the above map at 0.20 deg spatial resolution (Figure 4, bottom-left) has been smoothed by performing a bilinear interpolation. The resulting XCO2 distribution map (Figure 5) shows the characterization of Italian areas in terms of gas emissions/absorptions.

The detailed spatial analysis reveals sinks and sources of CO_2 (Figure 5) that well correspond to vegetated areas and densely inhabited areas, respectively. Specifically, the analysis of Figure 5 reveals a source area of CO_2 that mainly corresponds to the north Italian regions with more population and industries, in particular Lombardia, Piemonte and Veneto regions. Moreover, local sources are along the coast corresponding to: the city of Civitavecchia harbour area; the city of Naples with an overlapping of high density populated, industrial and active volcanic degassing areas; the Olbia harbour in Sardinia and along the north part of the Adriatic coast were many cities and industrial areas are present. CO_2 sinks areas mainly correspond to mountain massifs covered by dense vegetation and sparsely populated (eastern and western Alps, Liguria, central Italy, Calabria and north of Sicily). In other cases, sources of CO_2 do not correspond to any area with strong anthropization, such as the sources located on Asinara island of Sardinia, on south Sicily and central Alps. In the first two cases, the positive values areas are probably due to an influence of land/sea mask as they are not present in the map at spatial grid of 0.10 deg (Figure 4). The anomaly in central Alps could depend on the density of population towards the south, on a possible accumulation due to dominant winds or could be a false positive due to the smoothing effects on the jagged boundaries and coasts.

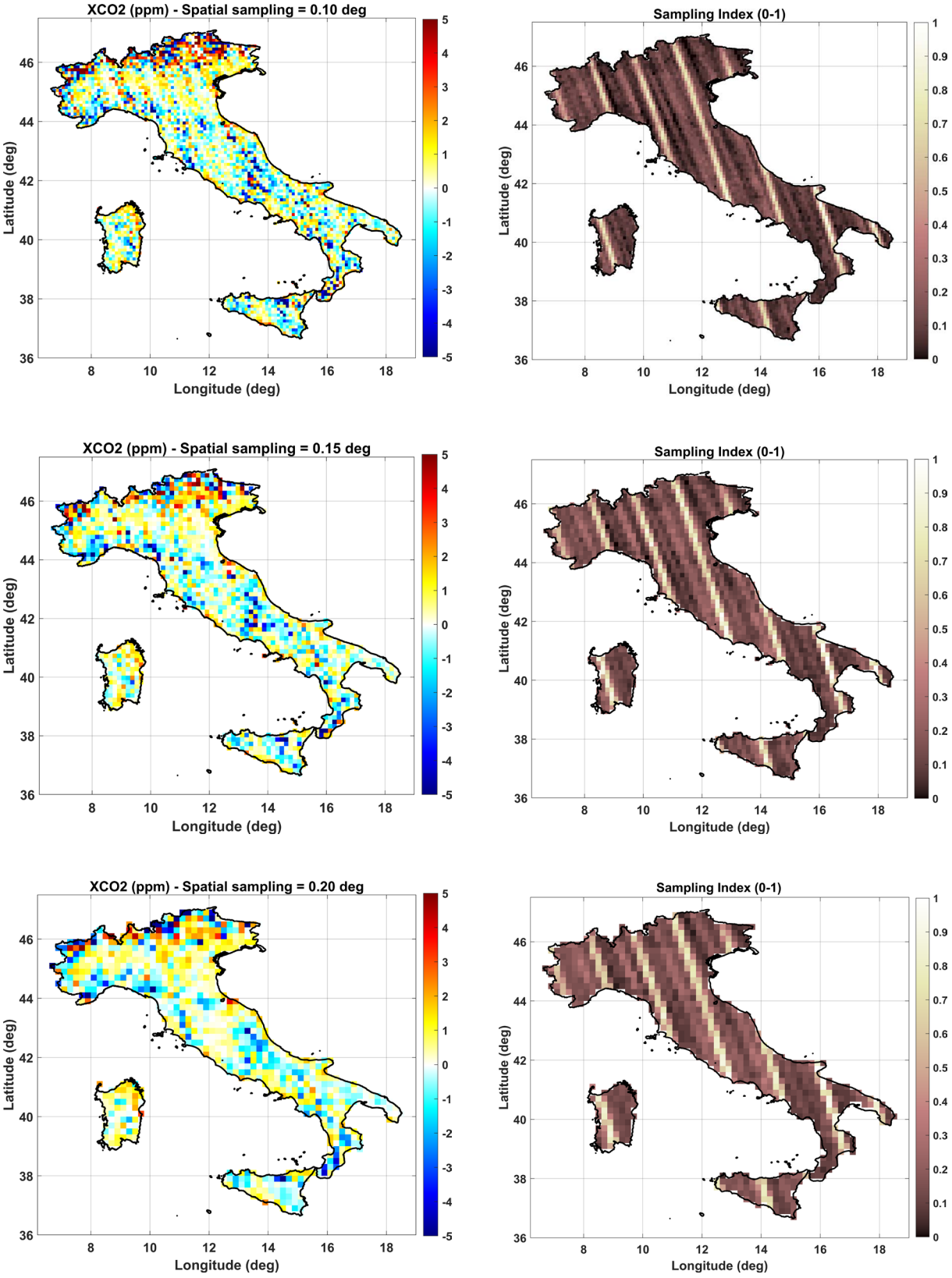

Figure 4. XCO2 (ppm) distributions at 0.10, 0.15 and 0.20 deg (left column: top, middle and bottom, respectively) and the corresponding Sampling Index maps (right column).

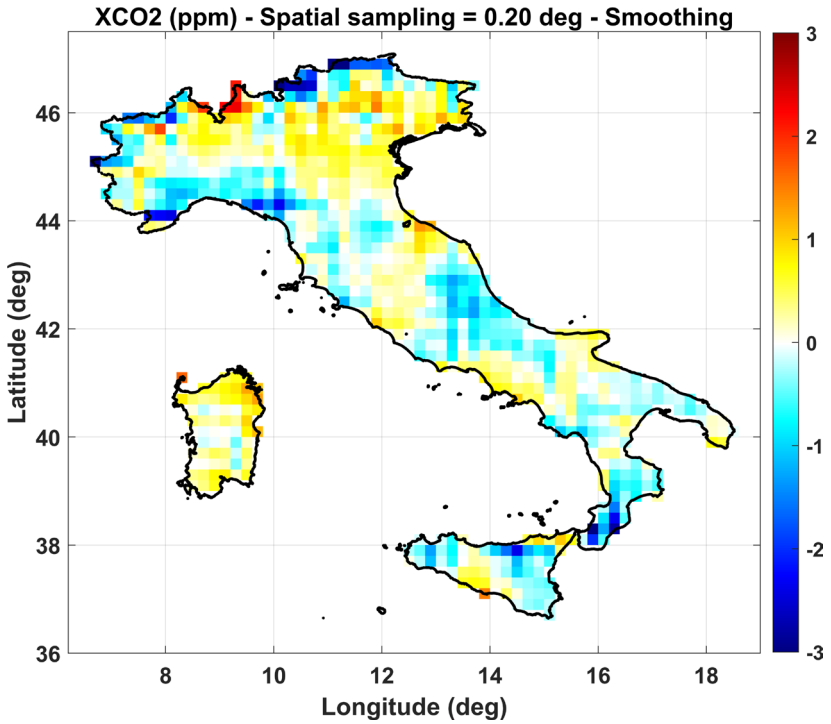

Figure 5. Smoothed XCO2 (ppm) enhancements at the spatial scale of 0.20 deg.

4. Conclusions

In this work, for the first time, 8 years of OCO-2 acquisitions over the Italian territory have been statistically analysed. After data reprocessing and compensating on temporal frequency of OCO-2 acquisitions over Italy, an increment of 21 ppm between 2015 and 2022 over land has been estimated. The seasonal behaviour and the main trend of CO_2 correspond to those achieved by the ECMWF model. A significant rate in the trend, between the end of 2019 and the beginning of 2020, shows an increase of about 6 ppm with a return to average values of the trend (3 ppm/year) in 2021 and 2022. This behaviour could be due to the COVID19 pandemic lockdown, occurred in the first months of 2020, slowing down the increment trend.

The detailed spatial analysis reveals that the north Italian regions, with more population and industries, are the source of CO_2, while sink areas of CO_2 mainly correspond to mountain massifs covered by dense vegetation, implying the fundamental role of vegetation as sink of CO_2. This work contributes to the European Union's Greenhouse Gas Monitoring Mechanism that requests countries to improve over time their estimates of emissions by sources and removals by sinks, following 2006 IPCC Guidelines for national GHG inventories and in line with the IPCC reporting principles of transparency, accuracy, consistency, completeness and comparability.

Data Availability Statement. OCO-2 data are available free of charge under the OCO-2 project license policy and can be accessed online at the official website https://search.earthdata.nasa.gov/search (accessed on 25 May 2023). The ECMWF data are published under a Creative Commons Attribution 4.0 International (CC BY 4.0).

Acknowledgements. OCO-2 data were produced by the OCO-2 project at the Jet Propulsion Laboratory, California Institute of Technology, and obtained from the OCO-2 data archive maintained at the NASA Goddard Earth Science Data and Information Services Center. The ECMWF data were generated using Copernicus Atmosphere Monitoring Service (2023) information.

References

Agustí-Panareda, A., S. Massart, F. Chevallier, S. Boussetta, G. Balsamo, A. Beljaars … and D. Wunch (2014). Forecasting global atmospheric CO_2, Atmos. Chem. Phys., 14, 11959-11983, doi:10.5194/acp-14-11959-2014.

Bartoletto S. and M.M. Rubio (2008). Energy transition and CO_2 emissions in Southern Europe: Italy and Spain (1861-2000), Global Environment, 1(2), 46-81(36), White Horse Press, https://doi.org/10.3197/ge.2008.010203.

Buchwitz, M., M. Reuter, O. Schneising, H. Boesch, S. Guerlet, B. Dils … and Y. Yoshida (2015). The Greenhouse Gas Climate Change Initiative (GHG-CCI): Comparison and quality assessment of near-surface-sensitive satellite-derived CO_2 and CH_4 global data sets, Remote Sens. Environ., 162, 344-362.

Corona, P., A. Barbati, A. Tomao, R. Bertani, R. Valentini, M. Marchetti … and L. Perugini (2012). Land use inventory as framework for environmental accounting: an application in Italy. iForest-Biogeosciences and Forestry, 5, 4, 204, doi:10.3832/ifor0625-005.

Crisp, D., B.M. Fisher, C. O'Dell, C. Frankenberg, R. Basilio, H. Bösch … and Y.L. Yung (2012). The ACOS CO 2 retrieval algorithm – part II: global XCO2 data characterization, Atmos. Meas. Tech., 5, 4, 687-707.

Cusworth, D.H., R.M. Duren, A.K. Thorpe, M.L. Eastwood, R.O. Green, P.E. Dennison … and C.E. Miller (2021). Quantifying global power plant carbon dioxide emissions with imaging spectroscopy. AGU Adv. 2021, 2, e2020AV000350, https://doi.org/10.1029/2020AV000350.

Del Bianco, S., B. Carli, M. Gai, L.M. Laurenza and U. Cortesi (2013). XCO2 retrieved from IASI using KLIMA algorithm, Ann. Geophys., 56, doi: 10.4401/ag-6331

IPCC (2007). Climate Change 2007: Synthesis Report. Contribution of Working Groups I, II and III to the Fourth Assessment Report of the Intergovernmental Panel on Climate Change. IPCC, Geneva, Switzerland, 104.

ISPRA (2018). National Greenhouse Gas Inventory System in Italy. March 2018, http://www.sinanet.isprambiente.it/it/sinanet/serie_storiche_emissioni

Le Quéré, C., R.M. Andrew, P. Friedlingstein, S. Sitch, J. Hauck, J. Pongratz … and B. Zheng (2018). Global Carbon Budget 2018, Earth Syst. Sci. Data, 10, 2141-2194, https://doi.org/10.5194/essd-10-2141-2018.

Loizzo, R., R. Guarini, F. Longo, T. Scopa, R. Formaro, C. Facchinetti … and G. Varacalli (2018). PRISMA: The Italian Hyperspectral Mission. In IGARSS 2018-2018 IEEE International Geoscience and Remote Sensing Symposium, 175-178, IEEE.

Massart, S., A. Agusti-Panareda, I. Aben, A. Butz, F. Chevallier, C. Crevoisier … and O. Hasekamp (2014). Assimilation of atmospheric methane products into the MACC-II system: from SCIAMACHY to TANSO and IASI. Atmos. Chem. Phys., 14, 6139-6158, doi:10.5194/acp-14-6139-2014, 2014.

Masson-Delmotte, V., P. Zhai, A. Pirani, S.L. Connors, C. Péan, S. Berger … and B. Zhou (2021). Climate change 2021: the physical science basis. Contribution of working group I to the sixth assessment report of the intergovernmental panel on climate change, https://report.ipcc.ch/ar6/wg1/IPCC_AR6_WGI_FullReport.pdf

Nassar, R., T.G. Hill, C.A. McLinden, D. Wunch, D.B. Jones and D. Crisp (2017). Quantifying CO_2 emissions from individual power plants from space, Geophys. Res. Lett., 44, 19, 10-045.

OCO-2 data access (2023) at: https://disc.gsfc.nasa.gov/datasets/OCO2_L2_Standard_11r/summary?keywords=oco-2

Petrescu, A.M.R., G.P. Peters, G. Janssens-Maenhout, P. Ciais, F.N. Tubiello, G. Grassi … and A.J. Dolman (2020). European anthropogenic AFOLU greenhouse gas emissions: a review and benchmark data, Earth Syst. Sci. Data, 12, 961-1001, https://doi.org/10.5194/essd-12-961-2020.

Romaniello, V., C. Spinetti, M. Silvestri and M.F. Buongiorno (2021). A Methodology for CO2 Retrieval Applied to Hyperspectral PRISMA Data. Remote Sens. 2021, 13, 4502, https://doi.org/10.3390/rs13224502.

Schneising, O., J. Heymann, M. Buchwitz, M. Reuter, H. Bovensmann and J.P. Burrows (2013). Anthropogenic carbon dioxide source areas observed from space: assessment of regional enhancements and trends, Atmos. Chem. Phys., 13, 5, 2445-2454.

Schwandner, F. M., M. R. Gunson, C.E. Miller, S.A. Carn, A. Eldering, T. Krings … and J.R. Podolske (2017). Spaceborne detection of localized carbon dioxide sources, Science, 358, 6360, eaam5782.

Solazzo, R., M. Donati, L. Tomasi and F. Arfini (2016). How effective is greening policy in reducing GHG emissions from agriculture? Evidence from Italy, Sci. Total Environ., 573, 1115-1124, https://doi.org/10.1016/j.scitotenv.2016.08.066.

Spinetti, C., V. Carrère, M.F. Buongiorno, A.J. Sutton and T. Elias (2008). Carbon dioxide of PuuOo volcanic plume at Kilauea retrieved by AVIRIS hyperspectral data, Remote Sens. Environ., 112, 6, 3192-3199.

Thorpe, A.K., C. Frankenberg, D.R. Thompson, R.M. Duren, A.D. Aubrey, B.D. Bue ... and P.E. Dennison (2017). Airborne DOAS retrievals of methane, carbon dioxide, and water vapor concentrations at high spatial resolution: application to AVIRIS-NG, Atmos. Meas. Techn., 10, 10, 3833-3850.

UNFCCC website (2023) at: https://unfccc.int/news/unfccc-25th-anniversary-climate-action-is-more-urgent-than-ever (last access on December 2023).

WMO (2019). United in Science Report, available at: https://public.wmo.int/en/resources/united_in_science (last access on December 2023).

Yoshida, Y., N. Kikuchi, I. Morino, O. Uchino, S. Oshchepkov, A. Bril ... and T. Yokota (2013). Improvement of the retrieval algorithm for GOSAT SWIR XCO2 and XCH4 and their validation using TCCON data, Atmos. Meas. Techn., 6, 6, 1533-1547.

***CORRESPONDING AUTHOR: Vito ROMANIELLO**,
Istituto Nazionale di Geofisica e Vulcanologia, Via di Vigna Murata 605, Roma, Italy